

International Journal of Multidisciplinary Research and Growth Evaluation.



CFD Simulation of Air Flow through Square Column

Nguyen Chi Cong ¹, Pham Minh Vuong ², Le Thi Minh Nghia ³, Bui Quoc Khoa ^{4*}

- ¹⁻³ Ho Chi Minh City University of Technology, Vietnam
- ⁴ Van Lang University, Vietnam
- * Corresponding Author: Bui Quoc Khoa

Article Info

ISSN (online): 2582-7138

Volume: 05 Issue: 06

November-December 2024 **Received:** 02-10-2024 **Accepted:** 06-11-2024

Page No: 955-966

Abstract

In this paper, the Large Eddy Simulation (LES) flow modeling technique is used to solve the Navier-Stokes equations. In this, the effect of the stress components from the small structures is modeled by the Smagorinsky flow model. This mathematical model is used for the flow through a square cylinder at two different Reynolds number conditions Re = 400 and Re = 22,000. The computed results of the average flow and the features of the multi-dynamic components are compared with the results obtained from the DNS (Direct Numerical Simulation) method and the k-ε model, demonstrating the benefits of this method. Simultaneously, these results also align well with the experimental results at the same Reynolds number conditions.

Air flows through a square cylinder with a side of 1 cm under standard conditions with a temperature of 2930K, atmospheric pressure, and a kinetic coefficient of 1.513 *10-5 m2/s. Reynols number is 22000.

DOI: https://doi.org/10.54660/.IJMRGE.2024.5.6.955-966

Keywords: Smagorinsky Model, turbulent flow simulation, Reynolds number

For many years, flow modeling techniques using the Reynolds Averaged Navier-Stokes (RANS) equations along with models like k- ε or O- ω have been the only options to simulate and calculate flow in industrial settings. The benefit of using models based on the Reynolds Navier-Stokes average equations is that they involve relatively low computational effort and can be utilized with existing computing tools to obtain average flow characteristics. The drawback of these models is that the calculation's time response does not align with the actual flow's time response. Additionally, for these models, five to seven numerical terms are needed in the Reynolds-averaged equation, which depends on factors such as flow type, Reynolds number, and fluid type, each requiring different numerical terms.

Recently, the model-free Direct Numerical Simulation (DNS) approach to solving the Navier-Stokes equations has been examined for many types of flows. The benefit of this approach is that it precisely represents the time changes of the flow and the average values. The downside of the approach is that the computational expense is very high. Piomeli [1] calculated the amount of points needed for a three-dimensional moving flow in space using the DNS method at a scale of Re9/4. With the power of modern computers, this method can only simulate a few simple flows with low Reynolds numbers of several thousand. To solve the difficulties of the two flow modeling methods mentioned above, currently, the flow modeling method according to large structures (Large Eddy Simulation - LES) is being researched and used in many problems and in the future will be used in many flow calculation software. This LES method is based on the basic principle of directly calculating only large flow structures, while small structures will be modeled. Therefore, with the LES method, the modeling process only requires a moderate amount of calculation to be able to calculate large structures - structures that characterize the flow motion characteristics.

In this paper, the LES flow model with the Smagorinsky flow model [2] is applied to solve the problem over a square. The computational results will be compared with the experimental results by Lyn et al. [3, 4] and Durao et al. [5], showing the good agreement of the model with the experimental results.

This is the first part of the research on the LES method and is only applied to the flow through a simple square body, but it is also the foundation for the next research parts of this method for complex bodies applied in the industrial field later (flow through hydraulic machines, turbines, aircraft blades, etc.)

Theoretical basis

LES Turbulent flow simulation

In the LES shear modelling method, shear structures with larger excitations than the shear size are modelled directly, while those with smaller excitations than the shear size are modelled. To distinguish between large and small shear structures and to model the influence of small shear structures on large shear structures, a force function is applied to the Navier-Stokes equations. With this function, a physical quantity f in the equation will be divided into two parts; one filtered part \overline{f} , which represents the large-scale structure, will be calculated directly from the equation f', the other part, which represents the small-scale structure, will be modeled: $f = \overline{f} + f'$.

In which, the large-scale structure component \overline{f} has been filtered when applying a filter function as follows:

$$\overline{f}(\mathbf{x}) = \frac{1}{\prod_{i=1}^{3} \Delta_i(\mathbf{x})} \prod_{\Omega} \prod_{i=1}^{3} G_i \left(\frac{x_i - y_i}{\Delta_i(\mathbf{x})}, \mathbf{x} \right) f(\mathbf{y}) d^3 \mathbf{y}$$
(1.1)

Apply this equation to the continuity equation and the momentum equation:

$$\frac{\partial \overline{u}_i}{\partial x_i} = 0 \tag{1.2}$$

$$\frac{\partial \overline{u}_{i}}{\partial t} + \frac{\partial \overline{\left(u_{i}u_{j}\right)}}{\partial x_{j}} = -\frac{1}{\rho} \frac{\partial \overline{p}}{\partial x_{i}} + \frac{\partial}{\partial x_{j}} \left[\nu \left(\frac{\partial \overline{u}_{i}}{\partial x_{j}} + \frac{\partial \overline{u}_{j}}{\partial x_{i}} \right) \right]$$
(1.3)

The momentum equation after being applied will give rise to a quantity that models the nonlinear interaction of two velocity components in the directions i and j: u_iu_i .

One of the advantages of the LES method is that the kinetic equation after being translated can be written as the equation of motion of large-scale elements.

$$\frac{\partial \overline{u}_{i}}{\partial t} + \frac{\partial \overline{u}_{i}\overline{u}_{j}}{\partial x_{i}} = -\frac{1}{\rho} \frac{\partial \overline{p}}{\partial x_{i}} + v \frac{\partial^{2} \overline{u}_{i}}{\partial x_{i}\partial x_{j}} - \frac{\partial \tau_{ij}}{\partial x_{i}}$$

$$\tag{1.4}$$

In which: $\tau_{ij} = \overline{u_i u_j} - \overline{u_i} \overline{u_j}$, called the «substructure tensor», the influence of the velocity components of the small structure, which are not directly solved, on the velocity components of the large structure is modeled. This unknown quantity will be modeled.

In practice, the tensor under stress can be decomposed into its deviatoric stress components $\tau_{ij}^D = \tau_{ij} - 1/3\tau_{kk}\delta_{ij}$ and the effects of the main component on the pressure quantity

 $\overline{p}^* = \overline{p} + 1/3\tau_{kk}$. The resulting equation is of the form:

$$\frac{\partial \overline{u}_{i}}{\partial t} + \frac{\partial \overline{u}_{i}\overline{u}_{j}}{\partial x_{j}} = -\frac{1}{\rho} \frac{\partial \overline{p}^{*}}{\partial x_{i}} + \nu \frac{\partial^{2} \overline{u}_{i}}{\partial x_{j}\partial x_{j}} - \frac{\partial \tau_{ij}^{D}}{\partial x_{j}}$$
(1.5)

The system of equations and will be closed when the shear stress component is modeled by the shear stress model according to Boussinesq's hypothesis:

$$-\nabla . \tau^{D} = \nabla . \left(\nu_{T} \left(\nabla \overline{u} + \nabla^{T} \overline{u} \right) \right) \tag{1.6}$$

or:
$$\tau_{ii}^D = -2v_T \overline{S}_{ii}$$
 (1.7)

In which the smallest, V_T , will be calculated according to the Smagorinsky model [2].

$$\nu_T = \left(C_S \overline{\Delta}\right)^2 \left| \overline{S} \right| = \left(C_S \overline{\Delta}\right)^2 \left(2\overline{S}_{ij} \overline{S}_{ij}\right)^{1/2} \tag{1.8}$$

With C_s which It is called the Smagorinsky number. According to the theory of homogeneous and uniform motion, this number is determined $C_s \cong 0.18$. However, in many recent studies, authors have proposed to use $C_s \cong 0.15$.

The final equation has the form:

$$\frac{\partial \overline{u}_i}{\partial x_i} = 0 \tag{1.9}$$

$$\frac{\partial \overline{u}_{i}}{\partial t} + \frac{\partial \overline{u}_{i}\overline{u}_{j}}{\partial x_{i}} = -\frac{1}{\rho} \frac{\partial \overline{p}^{*}}{\partial x_{i}} + \left(\nu + \nu_{T}\right) \frac{\partial^{2} \overline{u}_{i}}{\partial x_{i}\partial x_{j}}$$
(1.10)

Thus the system of equations and will be closed by Smagorinsky's model.

Numerical calculation diagram

The Navier Stokes equations with the LES model are solved in a uniformly distributed computational domain in a Decart system by the finite difference method. The spatial scheme is a second-order exact central difference scheme. The temporal difference scheme is a Mac-Cormack scheme with two-step prediction and correction of second-order accuracy. The continuity and momentum equations are solved by the projection method of Najm *et al.* ^[6] to derive the Poisson equation. This Poisson equation is solved by the differential equation method to find the pressure, which is then introduced into the momentum and continuity equations to find the velocity components of the flow. The stability condition of the differential equation in this calculation is the condition CFL = 0.3 according to Pham *et al.* ^[7].

Boundary condition calculation configuration

The computational domain of the simple problem is a rectangular prism of dimensions L_x , L_y , L_z in three directions of velocity u_x , u_y , u_z in three-dimensional space as. The rectangular prism of dimensions D is placed parallel

to the axis Z of the rectangular prism. This prism problem is solved in three-dimensional computational space with

different numbers of solutions depending on the Reynolds number presented above.

Table 1: Ca	ılculation.	division and	timing	configuration
-------------	-------------	--------------	--------	---------------

	Reynolds	$D_{\rm (m)}$	$L_{\scriptscriptstyle X} \times L_{\scriptscriptstyle Y} \times L_{\scriptscriptstyle Z}$	$N_{X} \times N_{Y} \times N_{Z}$	$\Delta t_{(s)}$
	400	5.10-4	$_{24}D \times_8 D \times_{12}D$	192×128×96 ∐ 2,4.10 ⁶	10-6
Ī	22000	2.10-3	$_{15}D \times_7 D \times_{1,5} D$	400×256×32 □ 3,3.10 ⁶	10-5

The input variable condition of the problem is a uniform flow with velocity \vec{U}_0 . To create conditions for the flow to develop, the input velocity of the problem has a dynamic component of about 0.1%, this condition is also suitable for the conditions in reality as well as in experiments. The boundary conditions on the two sides of the perpendicular region with respect to the direction Y are symmetrical boundary conditions. The boundary conditions on the top and bottom sides of Z the perpendicular region with respect to

the direction Z are periodic because in this case we assume an infinitely long cylindrical geometry in the direction and this problem only solves a part of the cylindrical geometry. The output condition of the computational domain is the passive flow condition (whatever the flow inside is, the flow outside will have its properties preserved). And finally the flow condition on the diagram is the zero velocity components.

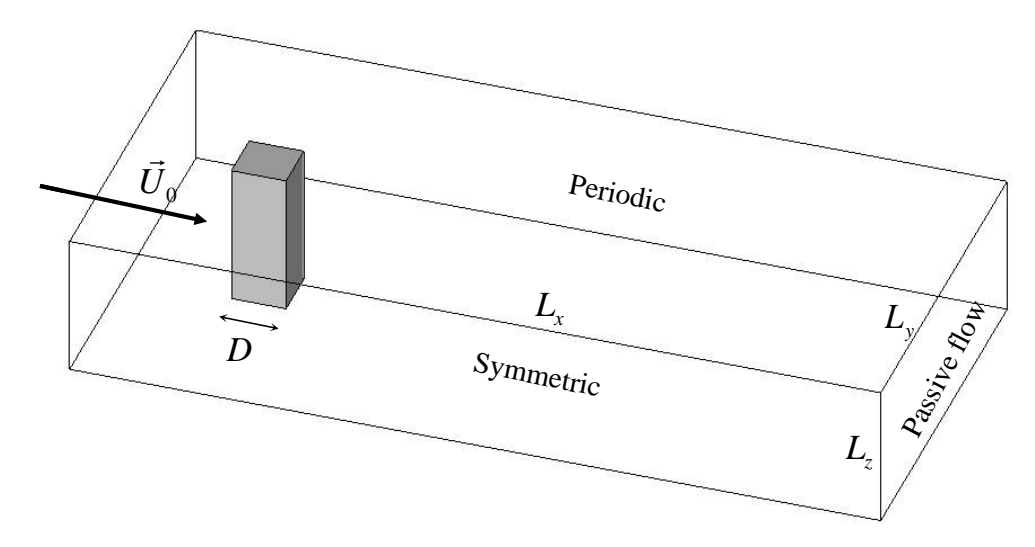


Fig 1: Computational configuration and conditions

Experience of Medium turbulent airflow and LES time Response Capability

Medium and turbulent airflow

As introduced in the previous section, in this paper the LES model is used to simulate the flow around a square cylinder in two cases with different Reynolds numbers. The effect of Reynolds number on the flow structure around the square cylinder will be discussed in the final section of the paper. In this section we will only discuss the flow through the diaphragm at Reynolds Re = 22,000 to be able to compare it with the experimental results as well as with other results calculated $k-\varepsilon$ by the Reynolds-averaged model. In this calculation, the flow around the cylinder is modeled in terms of the total time of the flow being 0.4s, of which the first 0.1s is the time required for the flow to reach a steady state from

an initial velocity of zero. The remaining time 0.3s is the time that the current has reached a steady state, and the average value is calculated from the average of all the values in the 0.3s steady state of the current.

The mean velocity in the flow direction (direction X) on the symmetric plane of the cylinder is shown in Fig. The results calculated by the LES model are also compared with the experimental results at the same Reynolds number condition Re = 22,000 performed by Lyn $et\ al.\ ^{[3,4]}$ and Durao $et\ al.\ ^{[5]}$. This comparison shows that the results calculated by the LES model are in close agreement with the experimental results of Lyn $et\ al.\ ^{[3,4]}$ in the front part of the figure. The back part of the figure shows a difference of about 5% to 10% between the calculated and experimental results.

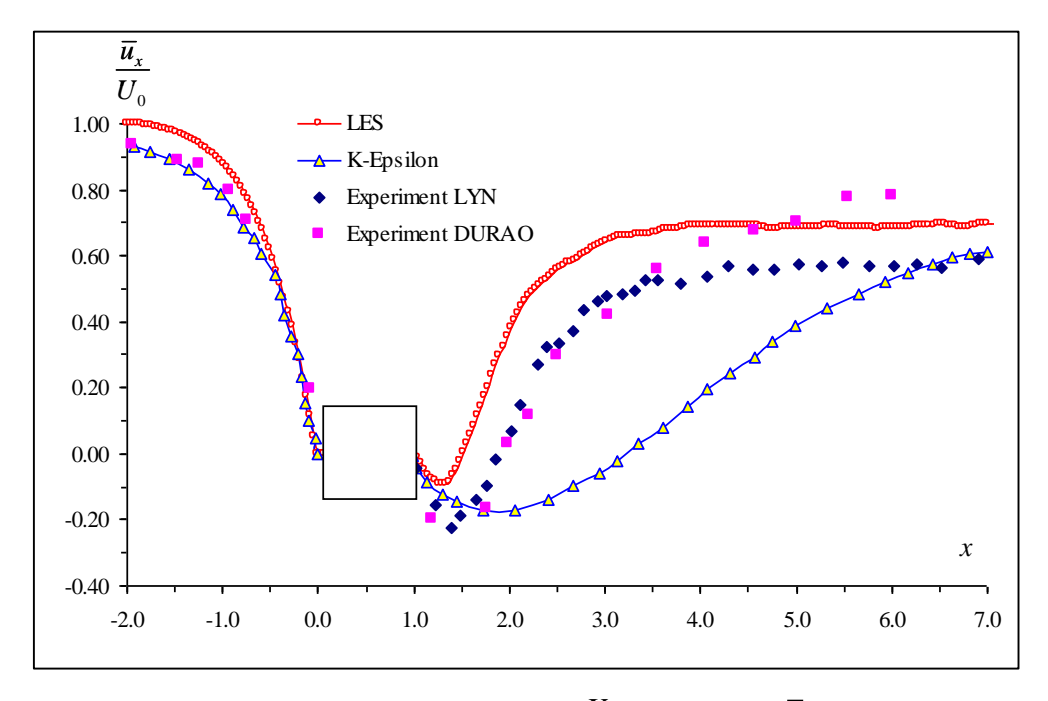


Fig 2: Distribution in the direction X of mean velocity \overline{u}_x

In this case, if we compare the results calculated by the LES model $k-\mathcal{E}$ applied to the Reynolds Navier Stokes average equation with the experimental results, there is a very large difference of up to 50% in the velocity part behind the image. While the velocity part in front of the image $k-\mathcal{E}$ calculated from the LES model and the experimental results are almost the same. This is also easily explained because the LES model is used to simulate and respond well over time so that it can accommodate the very large velocity variations after

the deformation caused by the Von-Karman vortices. While the model $k-\varepsilon$ applied to the Reynolds average equation has a poor time response (due to averaging the equation), it can only give good results for the pre-rotation velocity (because there is little noise) and significant errors for the post-rotation velocity, where there is a significant noise component. This will be discussed in more detail in the following section.

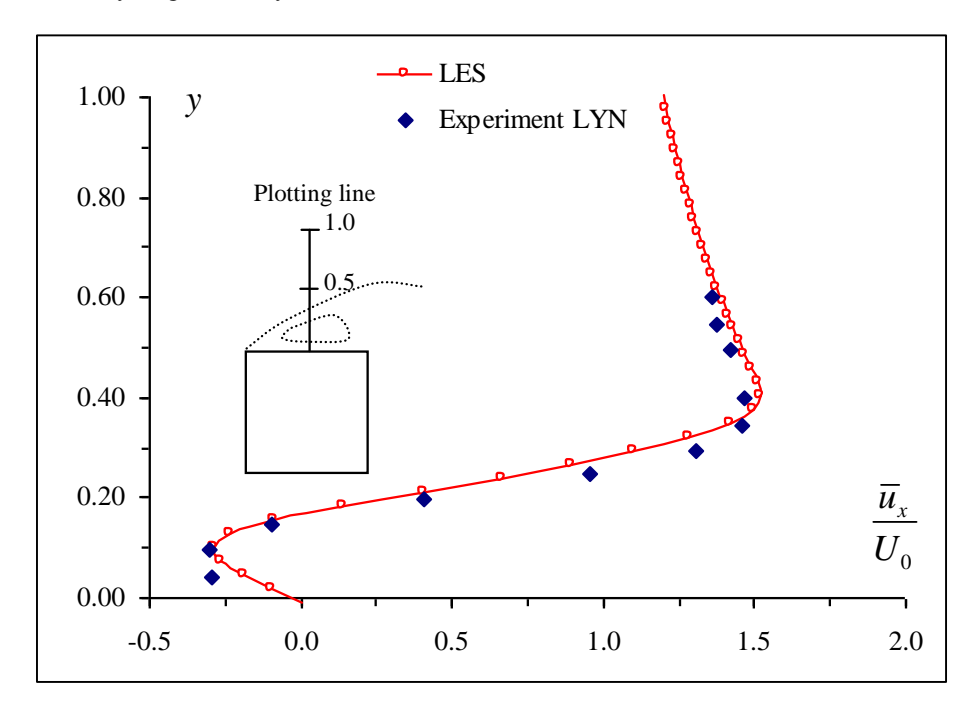


Fig 3: The distribution Y of the mean velocity curve on the upper surface \overline{u}_x

Another result in a relatively complex region is also presented, which is a square rotation on both sides, to show the adaptation of the LES model. This rotation lies on a very thin layer on both sides of the square. The LES calculation results are similar to the experimental results obtained by Lyn

et al. ^[3, 4] The y-direction average velocity \overline{u}_x profile of Fig. 3 at point x = 0,5D a shows the adaptation of the LES model. Physically, the phenomenon of boundary layer separation of the trough layer near the shear wall creates a reverse flow in

this region $u_x > 0$ and the flow returns to normal $u_x > 0$ when y > 0, 2D. With the above comparisons of the average current, the LES method gives results close to the experimental results.

Not only for the average value but also for the currents or for

the idle currents the dynamic component plays a very important role. This dynamic component is represented by

the dynamic energy of the current: $k = \frac{1}{2} \left(\overline{u_x'^2} + \overline{u_y'^2} + \overline{u_z'^2} \right)$ on the symmetrical plane shown in Figure 4.

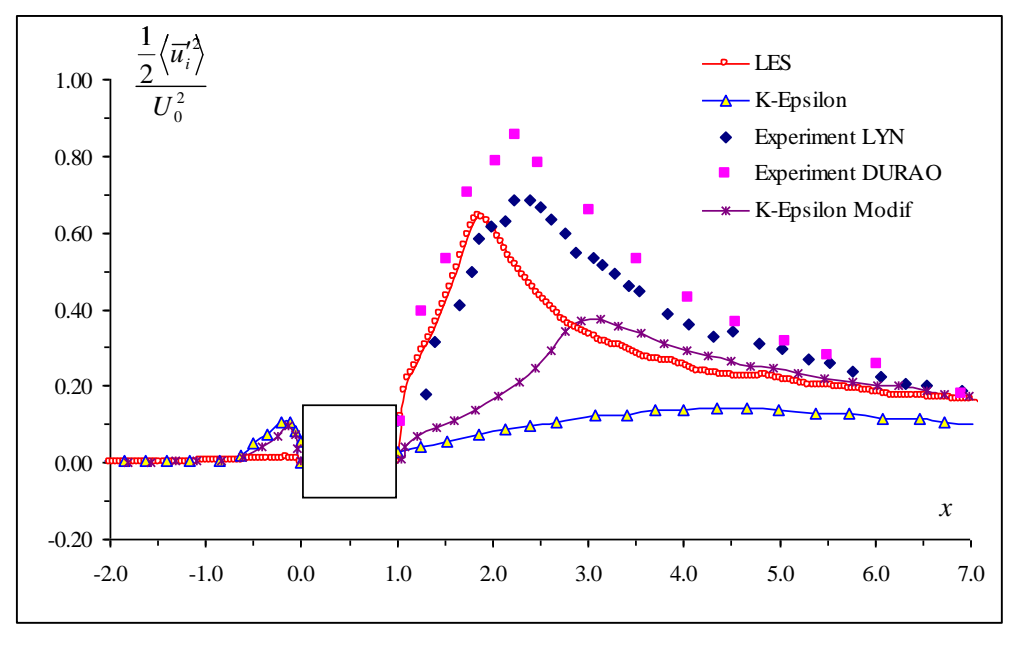


Fig 4: Divide the raft according X to the direction of the gate.

The calculated results of the dynamic response using the LES method are consistent with the experimental results by Lyn et al. [3, 4] and by Durao et al. [5]. Once again the comparison of the model $k - \varepsilon$ with the calculated results of the kinetic energy obtained from the multi-velocity components behind the image shows the limitations of the model $k - \varepsilon$ with both non-uniform flows and kinetic flows. In this case, the calculated result of the dynamic force by the model $k - \varepsilon$ by Franke and Rodi [8] after the regression only achieved the largest value of about 0.1 while the experimental results as well as the results calculated by the LES method were in the range $0.6 \div 0.7$ shown in Figure 4. Even with the corrected model $k - \varepsilon$ by Lamder and Kato [9], this value only achieved about 0.4. Thus, in terms of mean and dynamic range, the LES method has a remarkable agreement with the experimental results while the model $k - \varepsilon$ has a certain limited capability.

2.4.2- LES Time Response Capability

To investigate the variation of quantities with time, as well as with frequency, in this section the method of frequency spectrum analysis of velocity signals is applied to determine the frequency variation of the stream. Figure 5(a) shows the frequency spectrum at point A located at the position x = 0.5D and y = 0.75D within the lateral rotation region of the figure. The energy at this point has a maximum at frequency f = 115 hz and has the form of the energy of the free current. The value of this frequency corresponds to the Strouhal number $St = \frac{fD}{U_0} = 0.14$, which is the integer

frequency of the Von-Karman vortex after the rotation. Comparison with the experimental results of Lyn *et al.* [3, 4] with St = 0,132, Durao *et al.* [5] with St = 0,139 shows the compatibility of this calculation result.

The frequency spectrum of a point B located behind the hexagonal prism X = 11D, y = 0 is shown in Figure 5(b). At this point, the frequency spectrum has no maximum value as seen in the region near the hexagonal prism, and the slope of the frequency spectrum on the logarithm is -5/3. The slope value of -5/3 indicates a Kolmogorov structure in this directional region. This analysis shows the evolution of the flow from layer to layer, and it also shows the capture of the flow structures of the LES method.

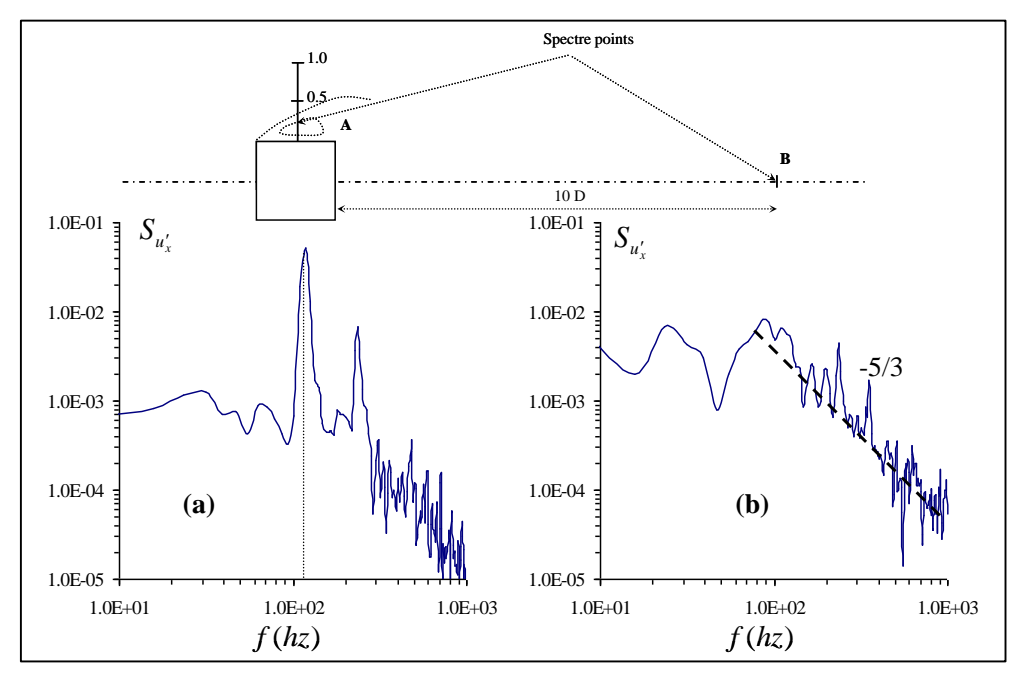


Fig 5: The energy density at two points A and B.

2.4.3- Reynolds flow structure

In terms of physics, in order to easily see the development of the flow structure, the calculation method and the representation of the turbulence field $\omega = \sqrt{\omega_x^2 + \omega_y^2 + \omega_z^2}$ are considered in this section. As mentioned in the introduction, the influence of the Reynolds number on the flow structure is also analyzed in this section, namely the two

Reynolds numbers $Re=22\,000$ and Re=400 . Figure 6(a) shows the is surface of the vortex field $\omega=5000\,(s^{-1})$ corresponding to $Re=22\,000$. In this case, in the region near the cylinder the flow structure is laminar with large structures. Farther behind the cylinder, these large structures overlap and are collapsed into small, laminar structures.

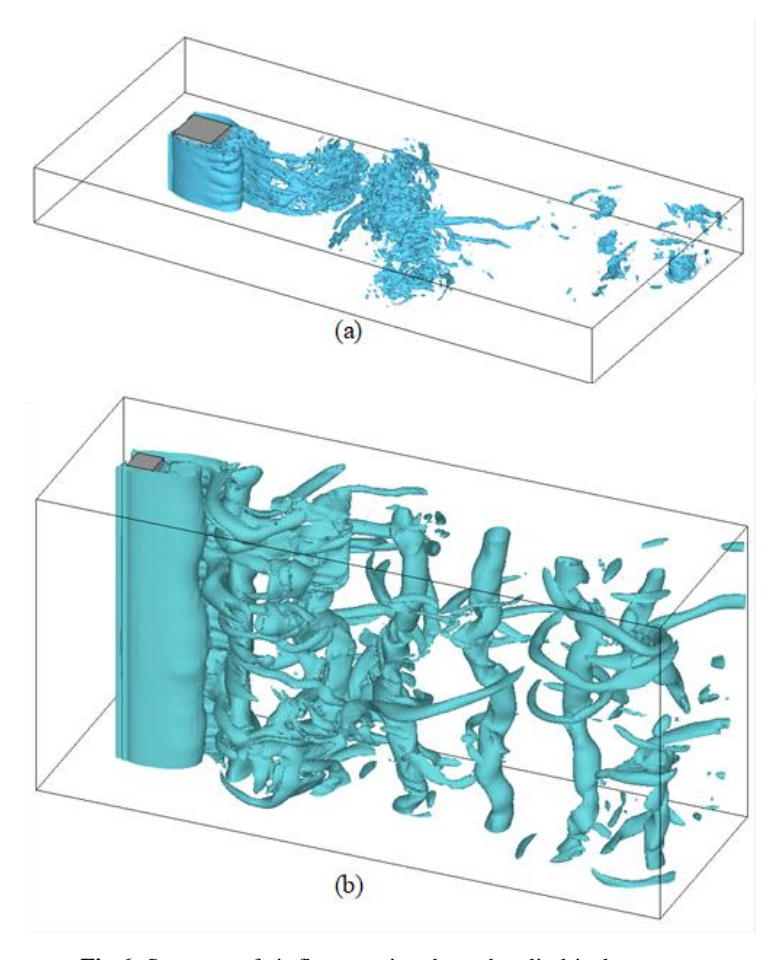


Fig 6: Structure of air flow moving through cylindrical structure

In contrast, in the case of the small Reynolds number Re = 400 shown in Figure 6(b) $\omega = 30000 (s^{-1})$, the near-circular flow structures are two-dimensional vortex tubes with longitudinal axis produced by the separation of the boundary layers. These two-dimensional vortex tubes are separated from the circular shape and deform into curved vortex structures in space as they move away from the circular shape. In addition, between these longitudinally curved vortex tubes, there are also vortex fibers entrained in the direction of flow caused by the deformation of the longitudinally curved vortex tubes. It is noteworthy here that, although they are entrained in each other, these vortex structures are not crushed in the case Re = 22000; showing the structure of a laminar flow. This structure is also a laminar flow structure obtained from the direct solution of the Navier-Stockes (DNS) equations by Lambalais et al. [10] together with Reynolds.

Result Experirencial model

Air flows through a square cylinder with a side of 1 cm under standard gas conditions with a temperature of 293^{0} K, atmospheric pressure, and a kinematic viscosity coefficient of $1.513*10^{-5}$ m²/s. Reynols number is 22000.

The drag coefficient is defined as follows:

$$C_D = \frac{F_D}{\frac{1}{2} \rho_{\infty} V_{\infty}^2 H}$$

In there:

 C_D the drag coefficient

 F_D air resistance

 ρ_{∞} kinematic viscosity coefficient

 V_{∞} velocity of air flow

H size of square cylinder

Set up the calculation domain with the following dimensions as shown in the figure:

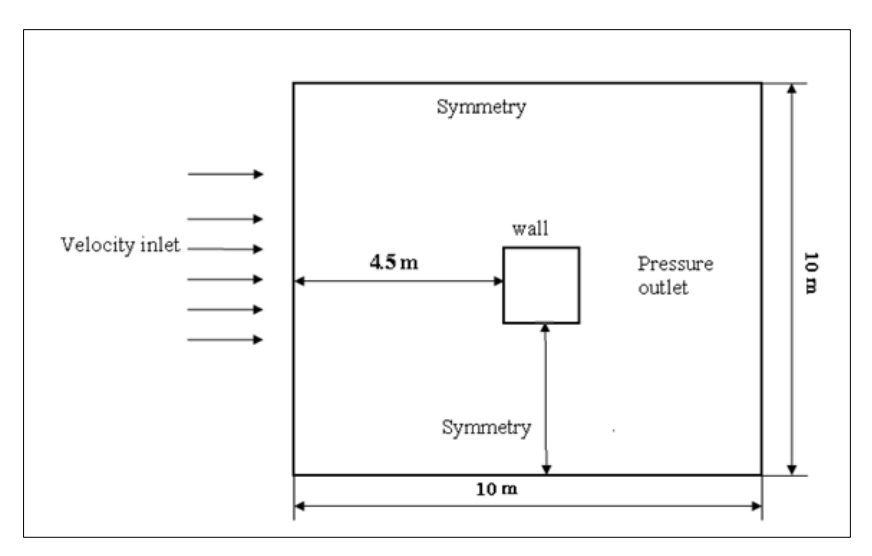


Fig 7: Dimensional parameters in the calculation model and boundary conditions

3.2. Discretized model of computational domain

After building the cylinder and the survey area, we use the Gambit tool to discretize the calculation area.

To simulate the flow through a cylindrical object accurately, we need to pay attention to the mesh density, the density of the mesh affects the calculation results. In the solid wall area, the fluid changes greatly, so we need to divide the mesh here more finely, to see the change of the flow clearly. The finer the mesh, the clearer the simulation, thereby seeing the change of the flow.

The cylindrical object, placed fixed in a natural environment with air flowing through, should be suitable for the properties of the fluid flow.

The calculation area is divided according to an unstructured mesh, triangular type.

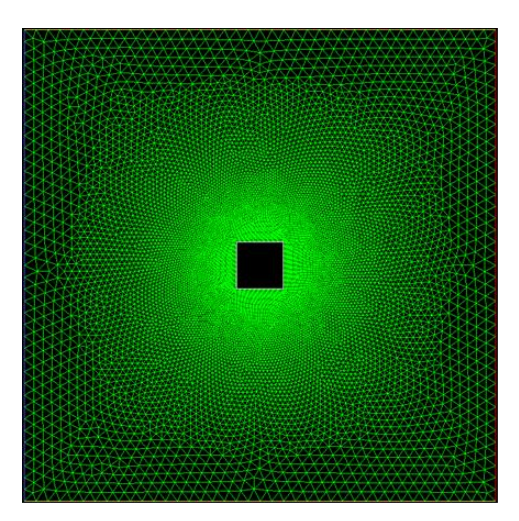


Fig 8: Discrete spatial computation on Gambit

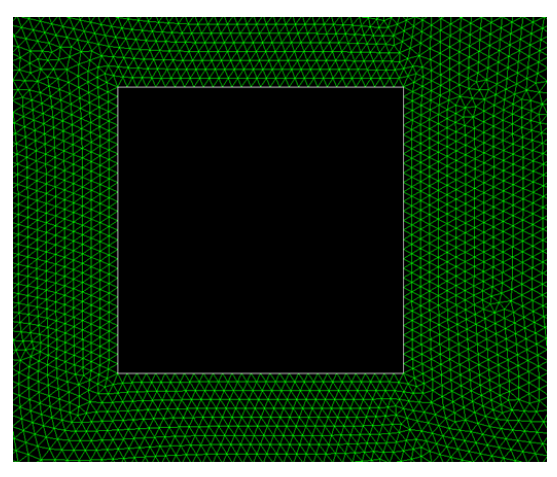


Fig 9: Mesh area near the cylinder boundary

3.3- Boundary conditions

The boundary conditions of the calculation domain are defined as input velocity boundary condition, output pressure condition, upper and lower surfaces symmetric boundary condition, square cylinder solid boundary condition. The values of these boundary conditions are shown in the following table:

Table 2: Input velocity boundary conditions

V (m/s)	\vec{r}	T(K)	I	L (cm)
39.358	(1,0,0)	293	5%	1

Table 3: Outlet pressure boundary conditions

P(Pa)	T(K)	I	L(cm)
9 81*104	193 774	5%	1

In which: I is the turbulence intensity, L is the characteristic

length. From the above parameters, we can calculate the turbulence kinetic energy k is 5.8 m²/s², the dissipation $^{\mathcal{E}}$ is 3286.5 m²/s³. After determining the boundary conditions, the step is to determine the algorithm diagram for the mathematical model. The basic equations are solved by the sequential solution method. Discretize the time domain according to the implicit diagram, choose the k - $^{\mathcal{E}}$ standard model and the solid-state fluid region is calculated according to the empirical functions. Use the SIMPLE algorithm diagram to calculate the pressure from the connection of the continuity equation and the momentum equation, the energy equation and the two characteristic equations of turbulence. The result of the problem will converge when the error of the problem is less than 10^{-5} .

3.4. Effect of number of mesh elements on calculation results:

Using Fluent software, we have the following result relating the number of mesh elements to the drag coefficient Cd:

Table 4: The relationship between the number of mesh elements and the drag coefficient Cd

No.	Number of mesh elements	Cd
01	22466	1.867
02	42600	1.867
03	56508	1.792
04	58776	1.838
05	65930	1.820
06	68300	1.806
07	69434	1.806
08	89120	1.795
09	94430	1.797

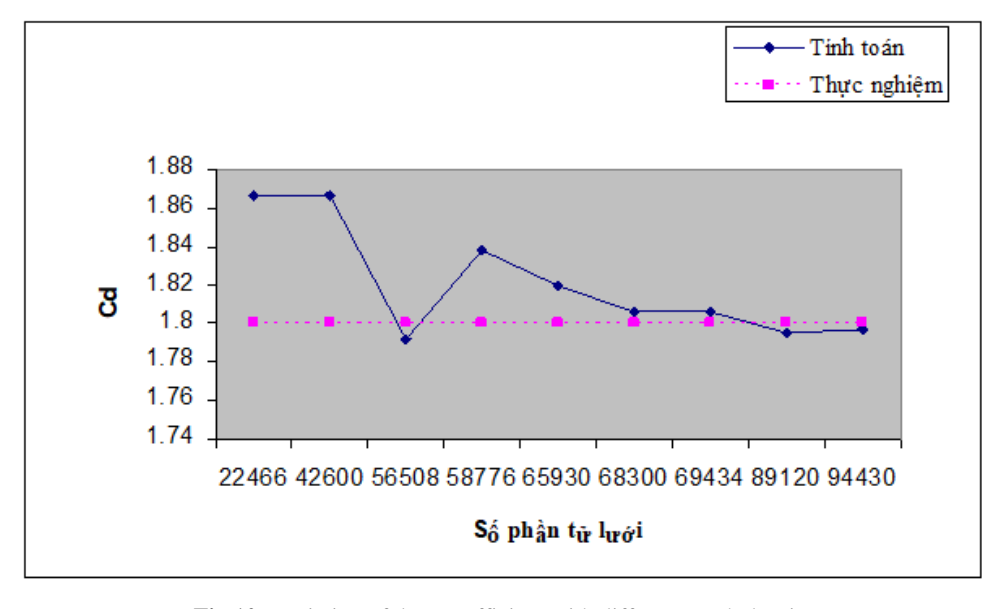


Fig 10: Variation of drag coefficient with different mesh density

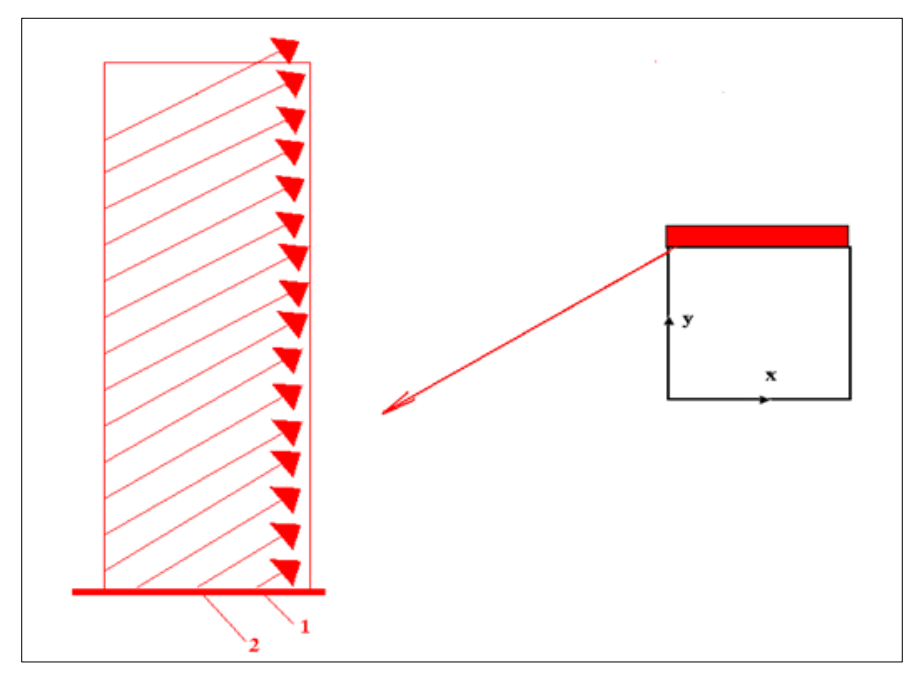


Fig 11: Check y⁺ of grid 68300

At the top surface of the cylinder in Figure 11, draw a vertical line. Output the velocity vector on this line, where u_1 and u_2 are the velocities on the solid wall of the cylinder and point 2 is the point close to the solid wall, the values y_1 and y_2 are the coordinates of point 1 and point 2.

Shear stress:

$$\tau_{_{w}} = \mu \frac{\partial u}{\partial y} \frac{u_{2} - u_{_{1}}}{y_{2} - y_{_{1}}} = 1.8549 \times 10^{-5} \frac{35.5598 - 35.5572}{0.00041} = 0.00011 (N/m^{2})$$

Impact velocity on solid wall:

$$\mu_{\tau} = \sqrt{\frac{\tau_{w}}{\rho}} = \sqrt{\frac{0.00011}{1.226}} = 0.0095 (m/s)$$

Distance to dimensionless solid wall:

$$y^{+} = \frac{\rho u_{\tau} \Delta y}{\mu} = \frac{1.226 \times 0.0095 \times 0.000408}{1.8549 \times 10^{-5}} = 0.25$$

So the y^+ value close to the solid wall is 0.25 < 5. So the mesh divided at the number of elements 68300 is reasonable.

3.5. Analysis of flow structure characteristics through a cylindrical object

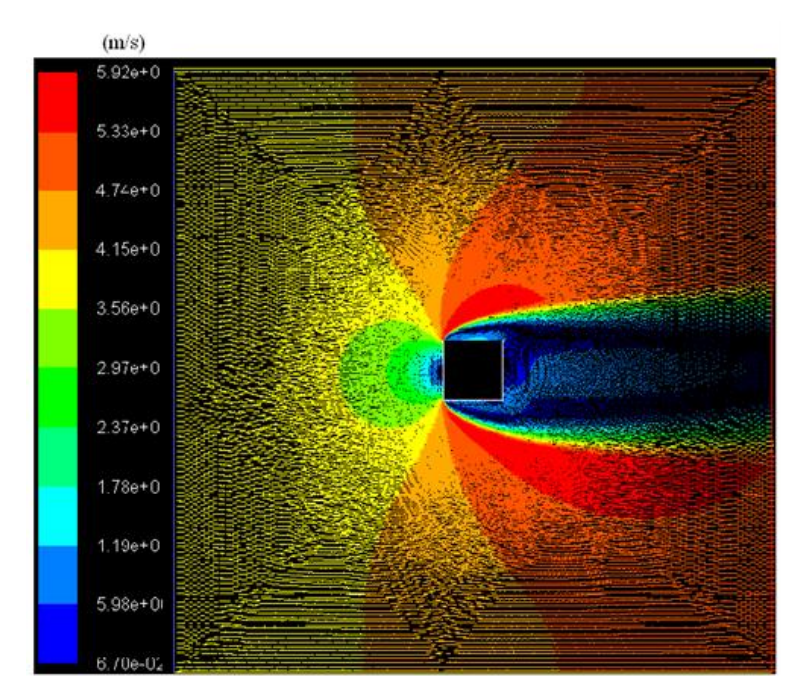


Fig 12: Velocity distribution of flow through square cylinder

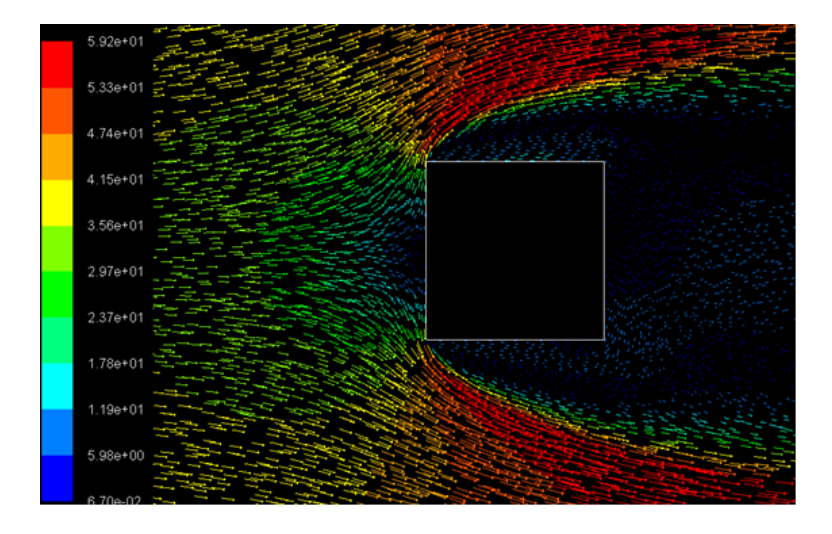


Fig 13: Zoom in on velocity distribution near square cylinder wall

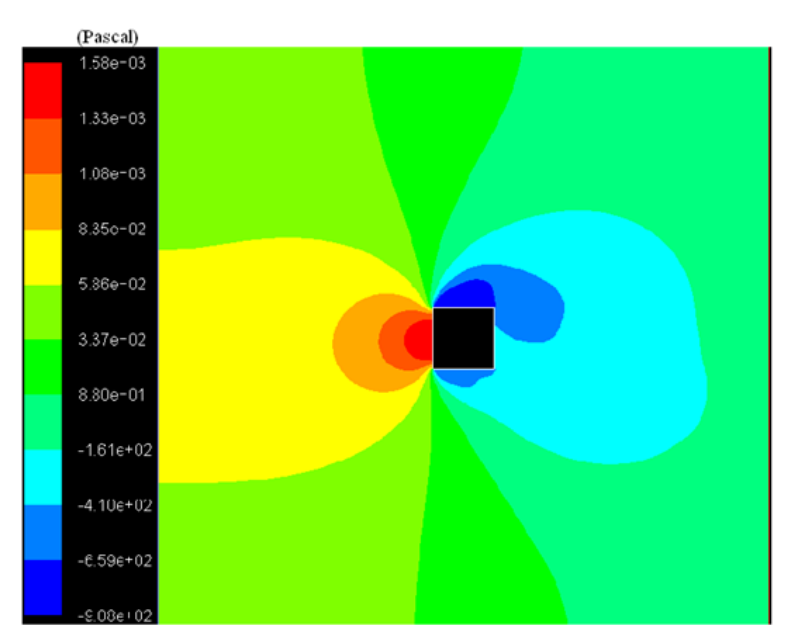


Fig 14: Pressure distribution through square cylinder

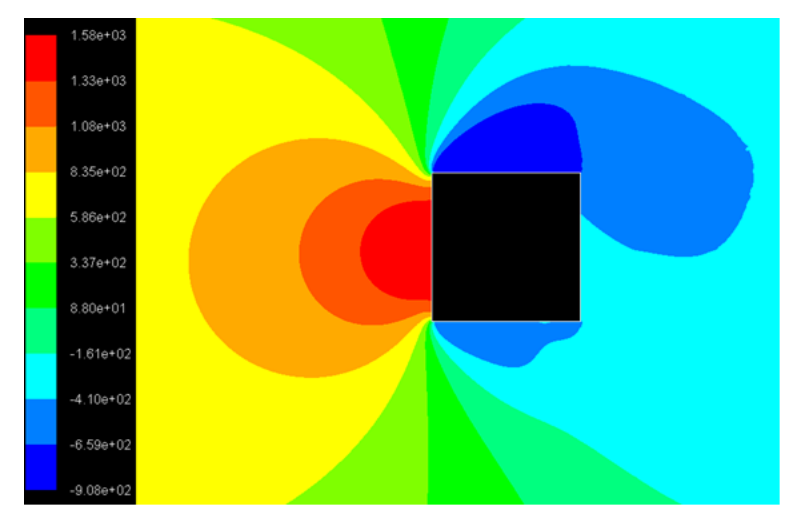


Fig 15: Zoom in on pressure distribution across square cylinder

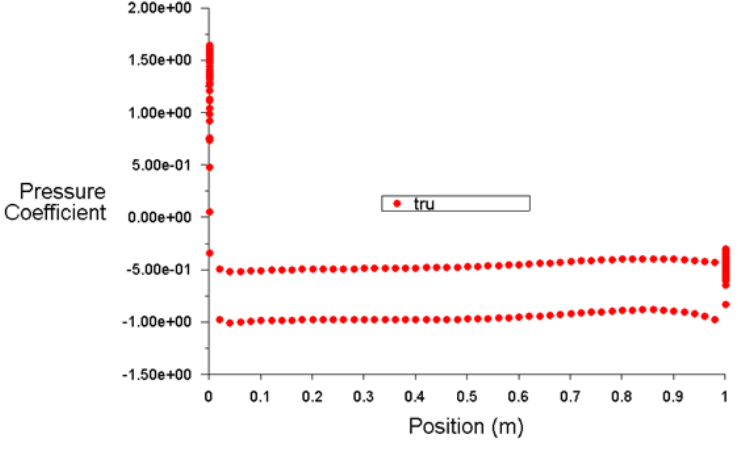


Fig 16: Pressure coefficient distribution on 2D cylindrical object

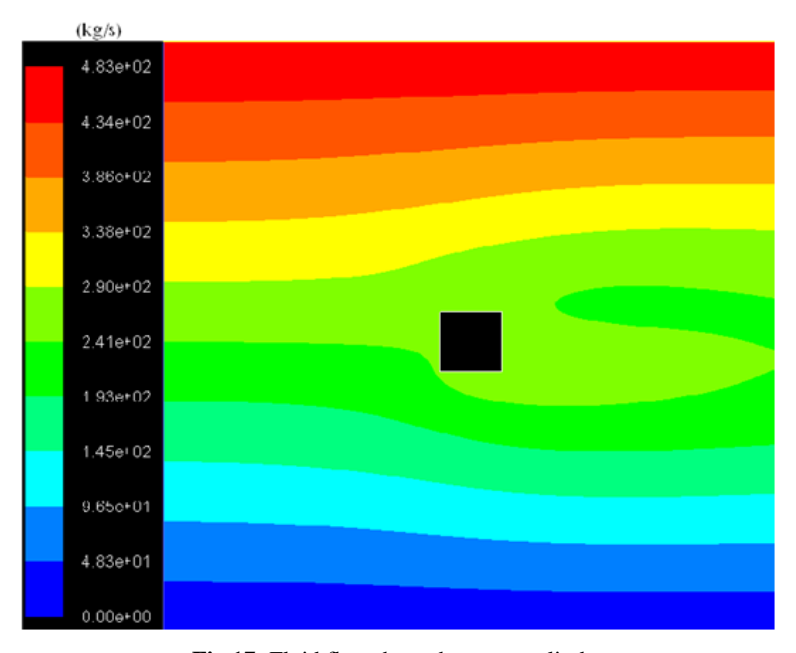


Fig 17: Fluid flow through square cylinder

Compare the drag coefficient C_D in the above calculation results with some other calculation methods and experimental

results in the case of flow through a 2D square cylinder (Re number in the range of 20000 - 22000).

Table 5: The drag coefficient CD in the above calculation results with some other calculation methods and experimental results in the case of flow through a 2D square cylinder (Re number in the range of 20000 - 22000)

Method	C _D	S_{t}	Grid
Basic Solver $(E_c = 0)$	1.82	0.130	100x90
$CVC (E_c = 0.001 - 0.002$	2.1 - 2.68	0.135 - 0.138	100x90
LES:			
Murakami	2.09	0.132	104x69x10
KAWAMU	2.58	0.15	135x78x20
UMIST2	2.02	0.09	140x81x13
RANS:			
_{KL - k -} €	1.79	0.142	100x76
RNG k - E	2.13	0.133	
TL - RSM	2.15	0.136	70x64
Exp.	1.92 - 2.2	0.136 - 0.138	

Conclusion

In this paper, the LES flow modelling method has been applied to solve the square envelope flow problem in two different Reynolds numbers. The results show the adaptability of the LES flow modelling method to the

experimental data in terms of both mean and time-varying values. The calculated results are also compared with some results of other authors using the model $k-\varepsilon$, showing the advantage of the best response time of the LES method. Despite its many advantages over the linear model $k-\varepsilon$, the

LES method using the Smagorinsky model still has many issues that need to be developed to better match experimental results. For example, the value of the constant $C_s = 0.15$ is chosen in most problems, but this value can be calculated if the LES method with the dynamic constant is used. And finally, what the authors want to say here is just the initial research part of the LES method that can give the flow through a square. But it is also a foundation for studying the application of this LES method to problems with complex shapes as well as industrial flow problems.

References

- 1. Piomeli U. High Reynolds number calculations using the dynamic subgrid-scale stress model. Physics of Fluids. 1993;A5:1484.
- Smagorinsky J. General circulation experiments with the primitive equations. Monthly Weather Review. 1963;91(3):99-164.
- 3. Lyn DA, Rodi W. The flapping shear layer formed by flow separation from the forward corner of a square cylinder. Journal of Fluid Mechanics. 1994;267:353-76.
- 4. Lyn DA, Einav S, Rodi W. A laser-Doppler velocimetry study of ensemble-averaged characteristics of turbulent near wake of a square cylinder. Journal of Fluid Mechanics. 1995;304:285-319.
- Durao DF, Heitor MV, Pereira JCF. Measurement of turbulent and periodic flows around a square crosssection cylinder. Experimental in Fluids. 1988;6:298-304
- 6. Najm HN, Wyckoff PS, Knio OM. A semi-implicit numerical scheme for reacting flow. Journal of Computational Physics. 1998;143:381-402.
- 7. Pham MV, Plourde F, Doan Kim S. LES simulation in a thin liquid film submitted to high thermal stress. ASME Summer Heat Transfer Conference; 2003 Jul 21-23; Las Vegas, NV, USA.
- 8. Franke R, Rodi W. Calculation of vortex shedding past a square cylinder with various turbulence models. Proc. 8th Symposium on Turbulent Shear Flows; 1991:189.
- 9. Lamder BE, Kato M. Modelling flow-induced oscillations in turbulent flow around a square cylinder. Proc. Forum on Unsteady Flow (FED). 1993;157:189.
- 10. Lamballais E, Sylvestrini SH. Direct numerical simulation of interactions between a mixing layer and wake around a cylinder. Journal of Turbulence. 2002;3:28.
- 11. Khoa BQ. Researching, designing, and manufacturing of the pollen bee vacuum dryer model. Ho Chi Minh City University of Technology; c2010.
- 12. Khoa BQ. Vietnam's renewable energy industry's approach to market development: Impact of Smart grid systems and renewable energy sources integration. International Journal of Multidisciplinary Research and Growth Evaluation; c2024. DOI: https://doi.org/10.54660/IJMRGE.2024.5.6.857-872.
- 13. Ngoc TM, Khoa BQ. Simulate energy in buildings according to LEED & LOTUS. Certification Science & Technology Publisher; c2023.
- 14. Ngoc TM, Khoa BQ. LEED rating system basis for green buildings. Certification Science & Technology Publisher; c2022.
- 15. Khoa BQ, Hay N, Duc LA, Tam PH. Optimization of the vacuum drying process for bee pollen using the R

- method. International Journal of Multidisciplinary Comprehensive Research; c2024. DOI: https://doi.org/10.54660/IJMCR.2024.3.6.51-56.
- Cong NC, Vuong PM, Nghia LTM, Khoa BQ. CFD simulation of convective airflow through a square cylinder. International Journal of Multidisciplinary Comprehensive Research; c2024. DOI: https://doi.org/10.54660/IJMCR.2024.3.6.57-62.